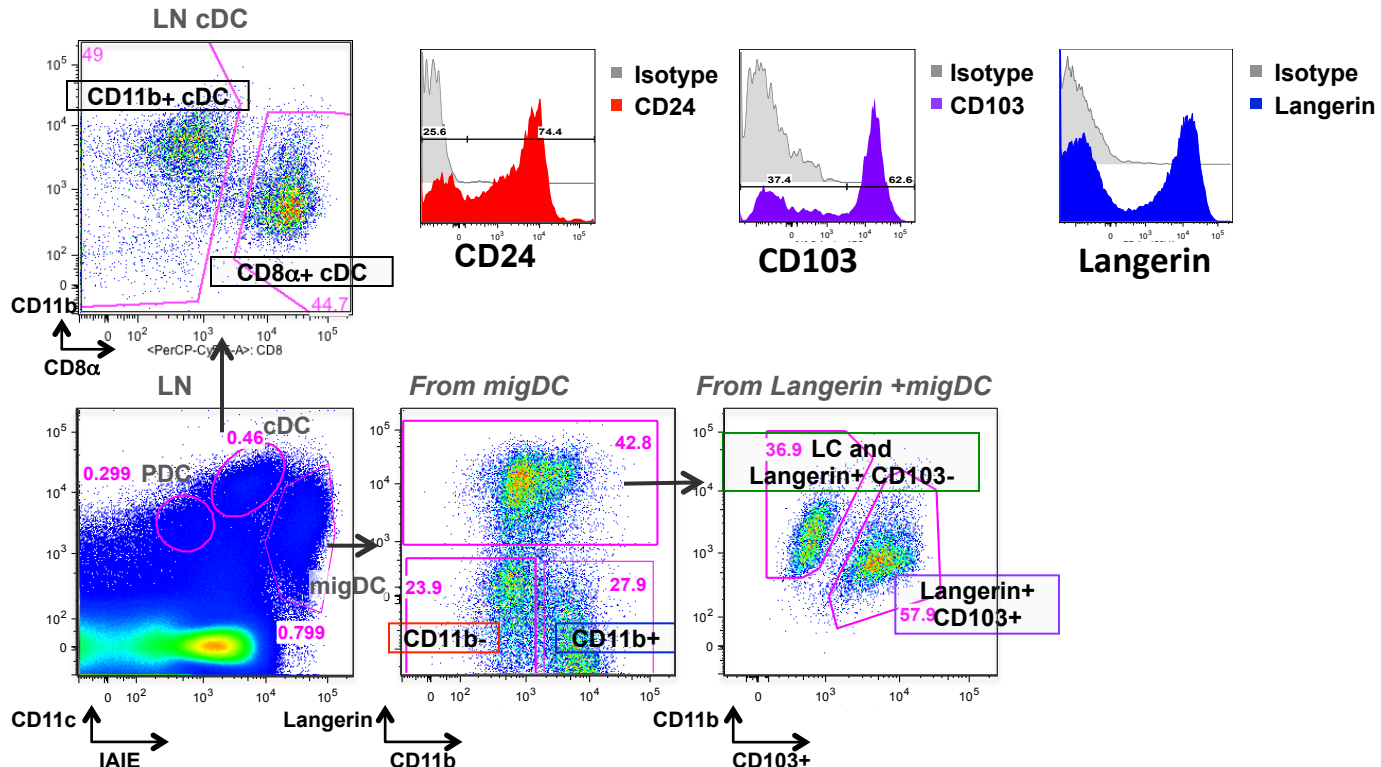
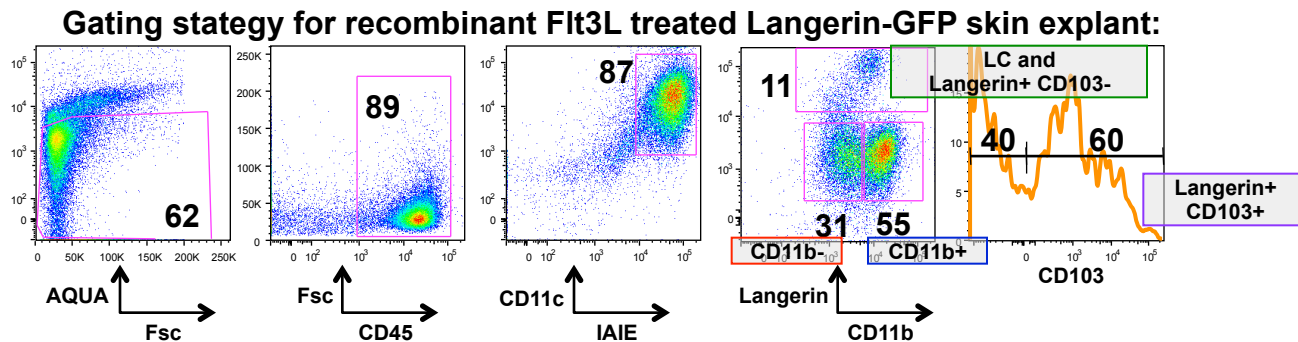
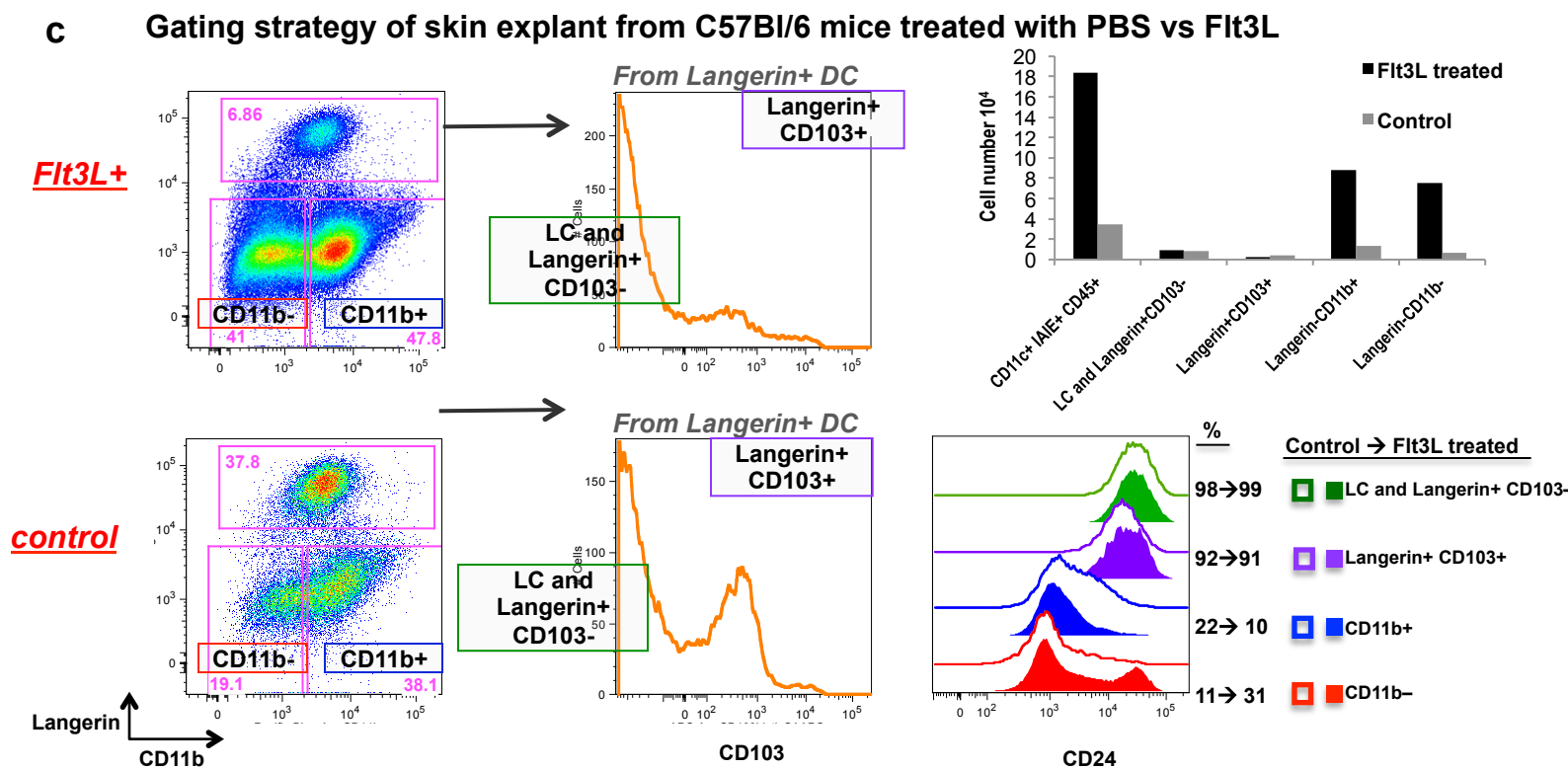
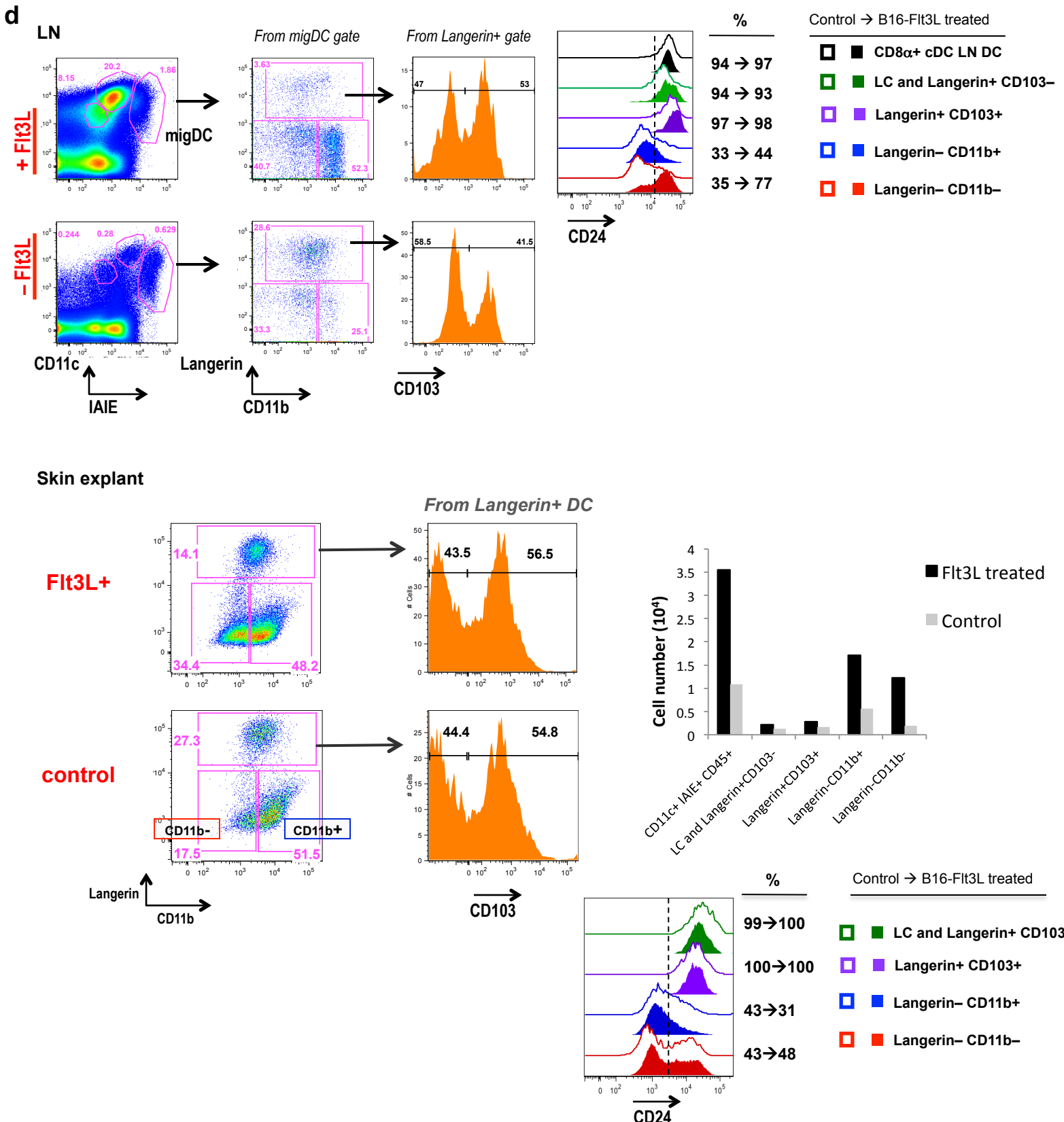


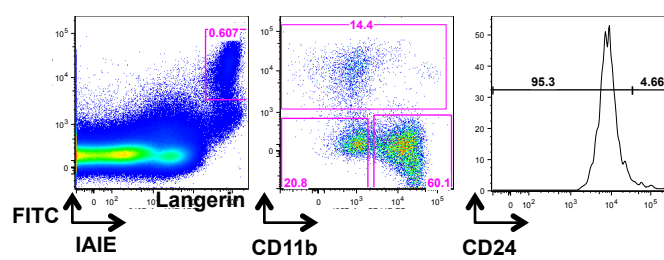
S1 Gating strategy for DC subsets in the: skin draining LN

a**b****c**

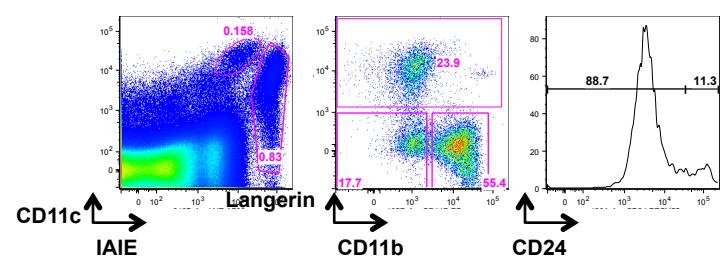
S1 Gating strategy of LN and skin explants from Flt3L-secreting B16 tumor treated mice vs. untreated controls:



S1

e

From FITC+ migratory DC gate



From all migratory DC gate

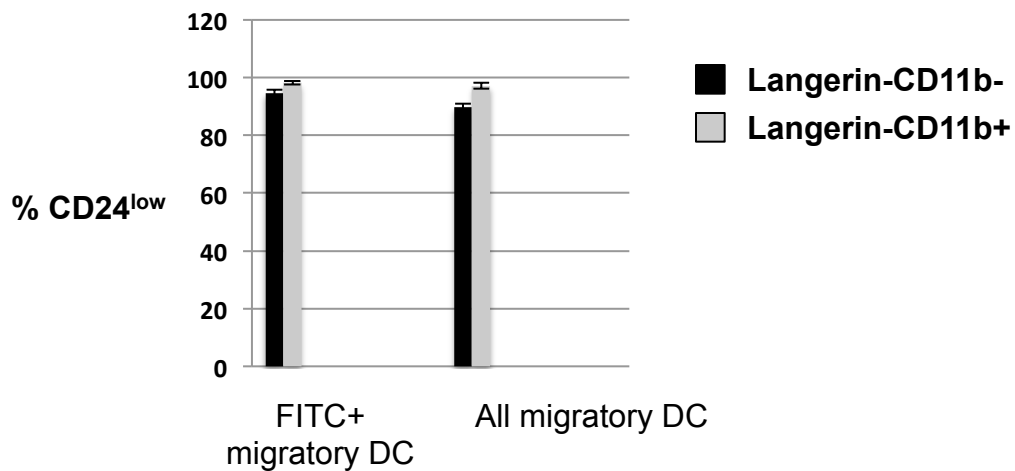


Figure S1. (A) Representative schematic of cDC and migDC subset gating in LN, (B) Representative gating schema for skin explant gating from Flt3L treated Langerin GFP mice and (C) skin explant gating from control and Flt3L treated C57BL/6 mice. For skin explants, ear halves were pooled from 3 individual mice and harvested at 72 hours. (D) LN and skin explant gating from C57BL/6 mice treated with B16-Flt3L tumors vs untreated controls. (E) During FITC painting the majority of the inflammatory infiltrate observed within the Langerin- gate and are CD24 low. (30 hours, n=3 mice, average percentage +/- standard deviation shown).

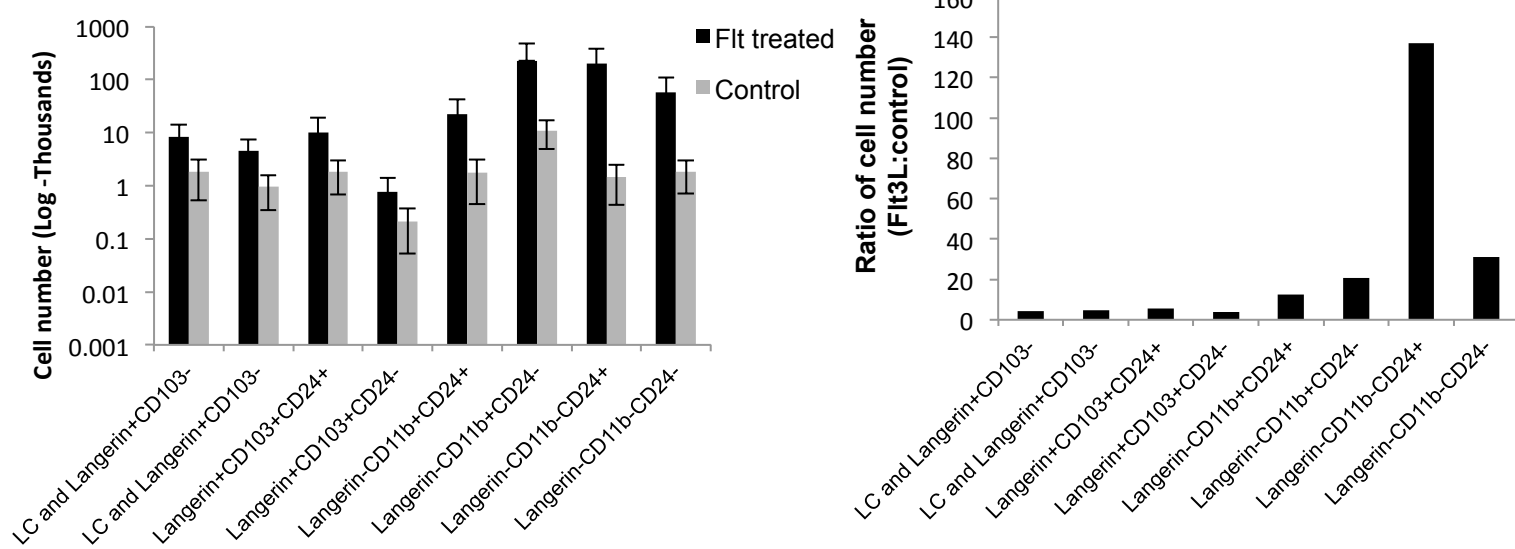
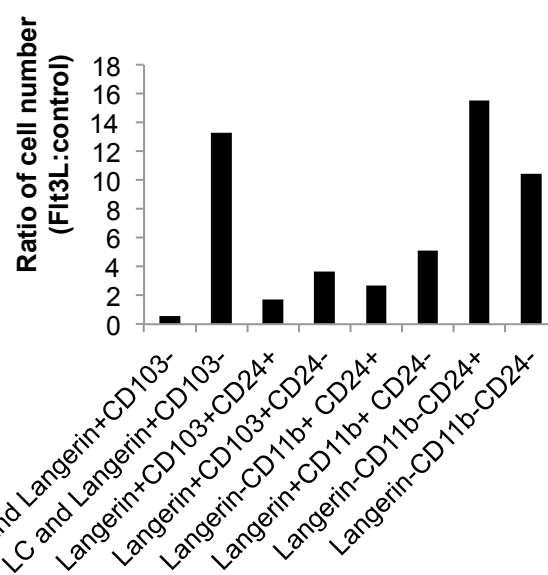
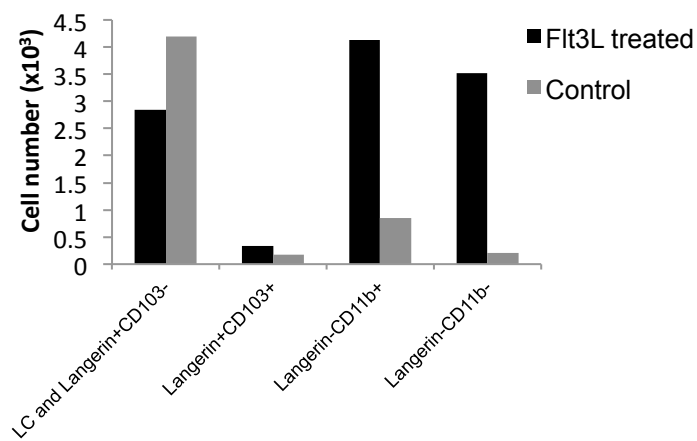
a LN:**b Skin explant:**

Figure S2. Quantitation of CD24⁺ and CD24⁻ migratory DC subsets from Flt3L treated and control mice (a. LN and b. skin explants). For LNs, the mean cell numbers (log) plus and minus the standard deviation from pooled axillary and brachial LNs are depicted. One of three replicate experiments shown.

S3

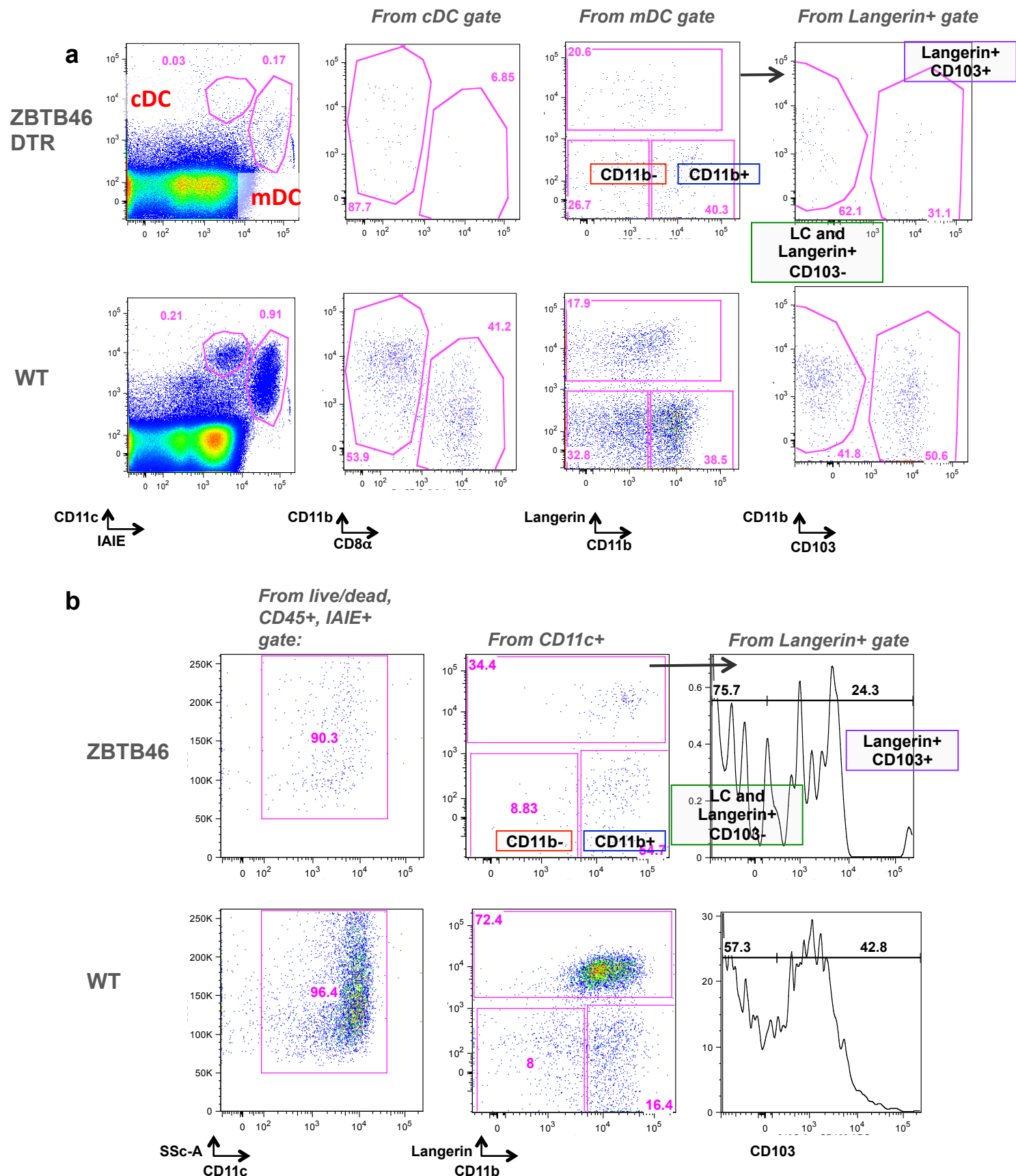


Figure S3. Representative flow cytometry gating of Zbtb46-DTR mice vs. C57BL/6 controls 24 hours post DT administration. DC from (A) skin draining LNs (B) skin explants.

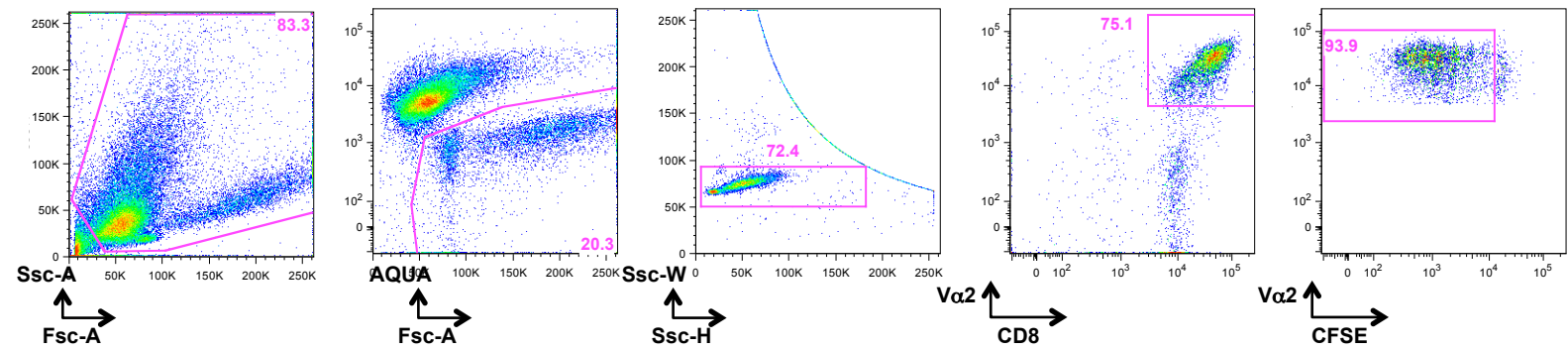
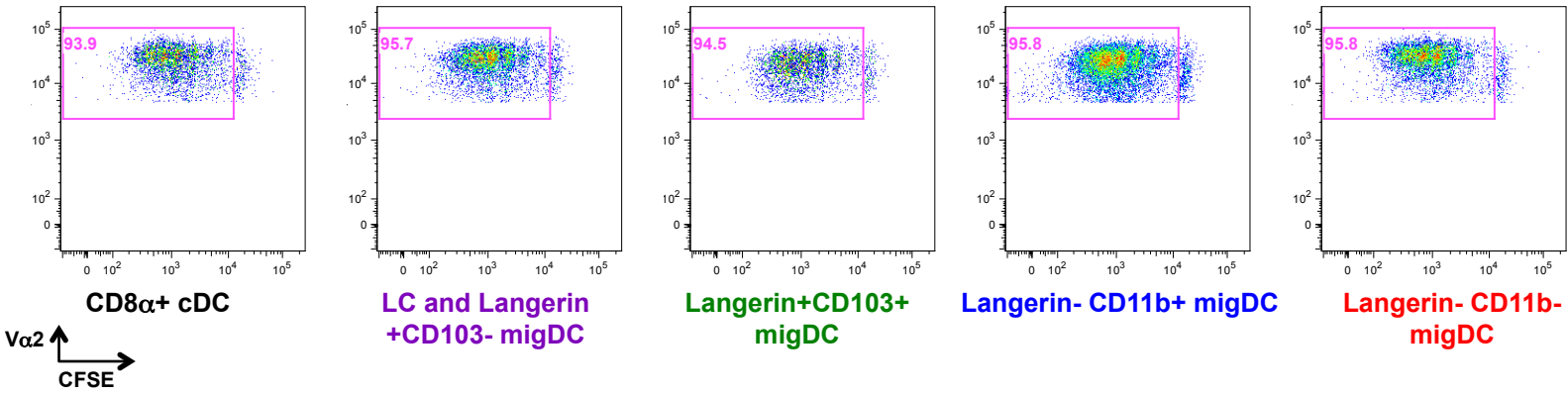
S4**Gating strategy for CFSE divided T cells:****CFSE^{lo} / divided:**

Figure S4. Representative gating of CFSE diluted OT1 (V α 2, CD8+) T cells cultured with DC subsets and OVA (one of three triplicate wells is shown per sample from duplicate experiments).